

Article

Distribution of Clay Minerals in Light Coal Fractions and the Thermal Reaction Products of These Clay Minerals during Combustion in a Drop Tube Furnace

Sida Tian ^{1,2,*}, Yuqun Zhuo ³, Zhonghua Zhan ^{2,4}, Xinqian Shu ⁵ and Zhizhong Kang ¹

¹ Key Laboratory of Condition Monitoring and Control for Power Plant Equipment of Ministry of Education, School of Energy, Power and Mechanical Engineering, North China Electric Power University, Beijing 102206, China; kzz@ncepu.edu.cn

² Department of Chemical Engineering and Institute for Clean and Secure Energy, University of Utah, 50 South Central Campus Drive, Salt Lake City, UT 84112, USA; zhonghuazhan@gmail.com

³ Key Laboratory for Thermal Science and Power Engineering of Ministry of Education, Thermal Engineering Department, Tsinghua University, Beijing 100084, China; zhuoyq@tsinghua.edu.cn

⁴ Reaction Engineering International, 746 E. Winchester St., Suite 120, Murray, UT 84107, USA

⁵ School of Chemical and Environmental Engineering, China University of Mining and Technology (Beijing), Beijing 100083, China; shuxinqian@126.com

* Correspondence: tiansida@ncepu.edu.cn; Tel.: +86-10-6177-3875; Fax: +86-10-6177-3877

Academic Editor: Vasily Novozhilov

Received: 6 April 2016; Accepted: 18 May 2016; Published: 1 June 2016

Abstract: To estimate the contribution of clay minerals in light coal fractions to ash deposition in furnaces, we investigated their distribution and thermal reaction products. The light fractions of two Chinese coals were prepared using a $1.5 \text{ g} \cdot \text{cm}^{-3}$ ZnCl_2 solution as a density separation medium and were burned in a drop-tube furnace (DTF). The mineral matter in each of the light coal fractions was compared to that of the relevant raw coal. The DTF ash from light coal fractions was analysed using hydrochloric acid separation. The acid-soluble aluminium fractions of DTF ash samples were used to determine changes in the amorphous aluminosilicate products with increasing combustion temperature. The results show that the clay mineral contents in the mineral matter of both light coal fractions were higher than those in the respective raw coals. For the coal with a high ash melting point, clay minerals in the light coal fraction thermally transformed more dehydroxylation products compared with those in the raw coal, possibly contributing to solid-state reactions of ash particles. For the coal with a low ash melting point, clay minerals in the light coal fraction produced more easily-slugging material compared with those in the raw coal, playing an important role in the occurrence of slugging. Additionally, ferrous oxide often produces low-melting substances in coal ash. Due to the similarities of zinc oxide and ferrous oxide in silicate reactions, we also investigated the interactions of clay minerals in light coal fractions with zinc oxide introduced by a zinc chloride solution. The extraneous zinc oxide could react, to a small extent, with clay minerals in the coal during DTF combustion.

Keywords: coal slugging characteristics; ash formation; aluminosilicate components; mineral matter distribution; density separation

1. Introduction

During pulverized coal combustion, entrained fly ash particles can selectively deposit on furnace walls and can produce slugging deposits, depending on their composition, temperature, atmosphere and other factors [1–6]. The prevention or reduction of boiler slugging is always a concern in the coal combustion research field. Minerals in coal are classified as either excluded or included, based

on the association of minerals within their coal matrices [7,8]. Light (low-density) fractions of coal contain less mineral matter, which is mostly held in its organic parts [7–11]. During the combustion of suspended coal particles, the included minerals can interact with organically bound mineral matter in the same coal particle and the char may promote oxygen-reduction reactions. These interactions can increase the production of low-melting substances. Therefore, studying the contribution of light coal fractions to ash deposition in furnaces to gain new insight on slagging formation mechanisms during coal combustion is necessary [7–12].

The main ingredients of ash deposition in utility boilers are aluminosilicates [6,13–16]. Recent experimental research on ash depositions has shown the importance of determining aluminosilicate components in ash to understand the slagging mechanism of coal blend combustion [3,15,17]. Clay minerals, classified as phyllosilicates, constitute much of the inorganic matter in coal and are the source of aluminosilicates in fly ash [1,2,4,14]. Therefore, to study the contribution of clay minerals to ash deposition in furnaces, investigating their distributions in light coal fractions and their thermal reaction products in the fly ash formation process is valuable.

Thermal reactions of clay minerals can involve dehydroxylation, self-transformations of the dehydroxylation products and combinations of the dehydroxylation products with extraneous metal cations [1,2,18]. In terms of pulverized coal combustion, products of these reactions may exist in fly ash depending on the combustion temperature. From a phase analysis viewpoint, thermal reaction products of clay minerals during pulverized coal combustion consist mainly of aluminosilicate glasses and mullite [1,4,13,19,20]. Chemical structures of substances dominate their thermophysical properties. In glass research, “NBO/T”, the ratio of non-bridging oxygen atoms (NBOs) to tetrahedrally coordinated cations, is often used to characterize the degree of polymerization in a melt or glass [20–22]. In the fly ash formation process, the modifier-rich substances produced by further reactions of dehydroxylated clay minerals have high NBO/T values and are easily melted, referred as the high NBO/T matter [18]. The high NBO/T matter represents easily-slagging material from the clay minerals in fly ash; the complexities of the chemical compositions and structures of amorphous aluminosilicate substances make it very difficult to directly examine high-NBO/T matter in fly ash.

Tian *et al.*, recently studied the characterization of high-NBO/T matter using acid-soluble fractions of aluminium in fly ash (denoted as soluble aluminium fractions) [18]. Aluminium in coal is basically derived from its clay minerals, which are the most abundant minerals in many coals. When aluminosilicates are treated by acids, the chemical structures of the aluminosilicates determine the solubility of the aluminium [22–26]. Tian *et al.*, analysed coal ash samples prepared at different temperatures in a drop-tube furnace (DTF) system using a chemical separation method with hot concentrated hydrochloric acid (denoted as boiling acid separation). The results showed that the acid-soluble aluminium fraction of DTF ash represented the total fraction of dehydroxylation products and high-NBO/T matter in the thermal reaction products of clay minerals in these coals. The dehydroxylation products decreased with increasing DTF temperature. At a DTF temperature of 1250 °C, the soluble aluminium fractions were correlated positively with high-NBO/T matter content in the thermal reaction products of the clay minerals in the two coals studied. In this investigation, the ash of light coal fractions was analysed using boiling acid separation to investigate the thermal reaction products of clay minerals in light coal fractions.

From a clay mineral reactions viewpoint, combination of clay minerals with active metal oxides can produce matter with higher NBO/T ratios [16]. Iron is one of major metal species that is found in coal, and ferrous oxide is an important metal oxide that can cause slagging. There has been considerable interest in how the association of clay minerals with ferrous oxide influences the combination of these substances during pulverized coal combustion [20,27,28]. However, iron in coal is often derived from several minerals, or even organic substances, and ferrous oxide is easily oxidized [5,20]. Therefore, it is difficult to elucidate the behaviour of ferrous oxide in the reactions of the clay minerals during pulverized coal combustion.

Zinc oxide has similar activity to ferrous oxide when reacting with silicate [29,30]. Both metal cations have approximately the same radius and metal-oxygen band energy, and their diffusion behaviours in silicate melts are very similar. The interaction of zinc oxide with clay minerals is an important reference for understanding ferrous oxide reactions with clay minerals.

When zinc chloride solutions are used as dense media to prepare light coal fractions, they carry small amounts of zinc chloride hydrate ($Zn_5(OH)_8Cl_2H_2O$). Zinc chloride hydrate can be converted into zinc oxide by heating at 200 °C [31]. When these light coal fractions are burned in DTFs, the zinc chloride hydrate decomposes to zinc oxide first, and the gaseous decomposition products, hydrogen chloride and water, rapidly diffuse into the flue gas flow. Thus, under these conditions, the role of zinc chloride hydrate is approximately equivalent to that of extraneous zinc oxide. Original, trace elemental zinc in coal can be ignored relative to the original iron in coal [32]; thus, the migration behaviour of the extraneous zinc oxide during combustion of light coal fractions is easy to determine.

In this study, light fractions of two previously studied Chinese steam coals [18] were prepared by density separation using a zinc chloride solution. The mineral matter in each light coal fraction was compared to the relevant raw coal. DTF ash from the light coal fractions formed at different combustion temperatures was analysed using boiling acid separation. The thermal reaction products of the clay minerals from these light coal fractions were compared to those from raw coal. Additionally, the influence of extraneous zinc oxide on the thermal reactions of clay minerals in light coal fractions is discussed in this report.

2. Materials and Methods

2.1. Materials

The two Chinese steam coals used to prepare the light coal fractions were SH coal (a high-volatile bituminous coal from the Shendong mining area) and WX coal (a low-volatile bituminous coal from Wuxiang County), which were characterized in a previous article [18]. SH coal has a low ash melting point with a high calcium content, while WX coal has a high ash melting point (Tables 1 and 2). Determination of fusibility of coal ash was determined according to the China Standard (GB/T 219-2008) [33]. Air is used as combustion atmosphere. The ash composition in Table 2 was determined using X-ray fluorescence (XRF). This has been achieved in an XRF apparatus (XRF-1800, Shimadzu, Kyoto, Japan) by means of rhodium (Rh) radiation.

Table 1. Proximate analyses (%) and ash fusion points (°C) of the coals (DT, deformation temperature; ST, soft temperature; HT, hemispherical temperature; FT, fluid temperature).

Sample	V _{ad}	A _{ad}	C _{ad}	M _{ad}	S _{t,ad}	Q _{gr,v} (J/g)	DT	ST	HT	FT
WX coal	13.9	27.9	57	1.2	1.55	25,092	>1450	-	-	-
SH coal	40.4	9.7	39.7	10.2	0.43	24,302	1130	1150	1170	1180

Table 2. Chemical compositions of the coal ash samples (%).

Sample	SiO ₂	Al ₂ O ₃	CaO	Fe ₂ O ₃	K ₂ O	MgO	Na ₂ O	SO ₃	TiO ₂	P ₂ O ₅
WX coal	51.32	36.78	2.48	4.2	0.5	0.39	0.14	1.94	1.32	0.53
SH coal	48.17	18.04	14.37	6.99	1.95	2.4	0.7	5.85	0.22	0.84

The powdered raw coal samples were prepared by first crushing raw coals to less than 3 mm with a jaw crusher and then grinding in a ball mill until 70% of the residue could pass through a 100 mesh sieve, which is similar to the coal fineness used in utility boilers [18]. The light coal fraction samples were prepared in a rotating centrifuge using a 1.5 g·cm⁻³ ZnCl₂ solution as a density separation medium [31]. For each separation, four plastic centrifuge tubes each containing 10 g of powdered coal and ~60 mL of 1.5 g·cm⁻³ ZnCl₂ solution were centrifuged at a rotor speed of 3000 rpm for 30 min.

The floating fraction on each liquid surface was removed, filtered, rinsed and dried in a vacuum oven at 105 °C. The light coal fractions were designated as “light coals” to distinguish them from the raw coal samples. The amounts of zinc chloride hydrate introduced by density separation were similar for the two light coals. The zinc contents in SH and WX light coals are 25.5 and 28.1 mg/g, respectively. After subtracting the zinc chloride hydrate, the remaining part of the light coal was the net light coal derived from the raw coal.

Some light coal samples require preheating to change the zinc chloride hydrate into zinc oxide for reliable analysis; the diffraction peaks of zinc chloride hydrate in X-ray diffraction (XRD) analysis hinder identification of silicate minerals in light coal, but those from zinc oxide do not [31]. For the preheating treatment, the light coal samples were heated in a muffle furnace at 200 °C using 45 mm × 22 mm porcelain boats (0.1–0.11 g light coal per boat) for 1 h. After subtracting the ZnO fractions, the remaining amount of the preheated light coal ash was the net light coal.

2.2. Combustion Experiments

Light coal combustion experiments were conducted in a DTF, as previously used to investigate raw coal combustion products [18]. The DTF tube had an inner diameter of 80 mm and a burning zone length of 1230 mm. The primary air, secondary air and cooling nitrogen flow rates were 110, 1000 and 625 g/h, respectively. The pulverized coal feed rate was ~0.1 g/min. The residence time of the fuels in the burning zone was ~1.5 s. The ash samples were collected at the base of the DTF using a water-cooled sampling probe. For both light coals, combustion experiments were conducted at three DTF temperatures: 1050, 1150 and 1250 °C. The collected ash products are designated as DTF ash.

Muffle furnace ash samples for these two light coals were also prepared by soak-heating for 1 h at 1050 °C after preheating for 1 h at 200 °C in a muffle furnace. The muffle furnace ash samples are herein designated as MF ash. With the long heating process, the MF ash was close to thermodynamic equilibrium, and the phase distribution was easier to identify using XRD analysis. In the phase analysis, the MF ash was compared to the corresponding DTF ash to show the extent of the thermal reactions of the clay minerals in the light coals during DTF combustion.

2.3. Sample Analysis

To determine the original mineral distributions in the light coals, low-temperature ash (LTA) from the preheated light coals was analysed by XRD. An oxygen plasma asher (K1050X, EMITECH, Lewes, UK) was used to prepare the LTA samples. The vacuum of the plasma asher is 0.8 mbar, and the temperature of low-temperature ashing is between 150 and 200 °C. An X-ray diffractometer (D8-Advance, Bruker, Karlsruhe, Germany) equipped with Cu-K α radiation (a wavelength of 0.15418 nm) and an array detector (LYNXEYE detector, Bruker, Karlsruhe, Germany) was used to measure the XRD patterns of the ash samples. Some preheated light coals were ashed using Chinese standard procedures (GB/T 212-1991) [34] to measure the amounts of major metal elements in the light coals. The ashing temperature was 815 °C. The 815 °C ash was subjected to digestion in a microwave oven (MARS5, CEM, Matthews, NC, USA) for ICP-AES analysis to identify the major metal elements. After subtracting the ZnO fractions, the remaining part of the 815 °C ash samples was the net light coal. Thus, the contents of major metal elements in the 815 °C ash of the net light coals were obtained.

The boiling acid separation and analysis methods employed for light coal DTF ash were the same those used for raw coal DTF ash [18]. A certain amount of DTF ash was mixed with 6.3 M hydrochloric acid in a 100 mL beaker and heated for 1 h on a 160 °C electric heating plate. After heat treatment, the mixture was filtered using a funnel with quantitative filter paper. The filtered liquid was saved to measure the dissolved element content, and the solid residues were dried for XRD analysis. An ICP-AES was used to identify aluminium and other key elements in the boiling acid solution. Each DTF ash sample was subjected to microwave digestion for ICP-AES analysis (Vista-MPX, Varian, Palo Alto, CA, USA) to measure the total aluminium content of the ash sample. The acid-soluble

aluminium fraction of each DTF ash sample was defined as the ratio of dissolved aluminium to total aluminium.

3. Results and Discussion

3.1. Mineral Matter Distribution in Light Coal

The mineral matter distributions in SH and WX raw coal were reported previously [18,35]. The clay minerals in both raw coals are primarily kaolinite and illite. However, the specific illite in the two fuels is different: in WX coal it is tobelite ($\text{NH}_4\text{Al}_2[(\text{AlSi}_3)\text{O}_{10}](\text{OH})_2$), and in SH coal it is muscovite ($\text{KAl}_2[(\text{AlSi}_3)\text{O}_{10}](\text{OH})_2$). To demonstrate the distributions of the minerals in these light coals, the XRD pattern of the LTA from each preheated light coal was compared to that of its raw coal. The major metal elements in the 815 °C ash of each net light coal were compared to those in the 815 °C ash of the relevant raw coal. As shown in the example in Figure 1, the mineral phases identified from the XRD pattern are listed in the top right corner of the spectrum. For every identified mineral phase, one or two distinct diffraction peaks are marked for clarity.

Figure 1 shows that the silicon-containing minerals in the WX light coal are quartz and clay minerals, as in the WX raw coal. The LTA samples of preheated light and raw coal have the same diffraction peak intensity ratio between kaolinite and tobelite, indicating that the mass ratio of kaolinite to tobelite in WX light coal is the same as it is in WX raw coal. Figure 1 also illustrates that the preheated light coal LTA contained no Zn-bearing minerals other than zinc oxide. The presence of zinc oxide demonstrates its stability during low-temperature ashing of the preheated light coal. The aluminium in the coal samples originated from the clay minerals. The aluminium content in the 815 °C ash of the WX net light coal is higher than that in the 815 °C WX raw coal ash (Figure 2). This result demonstrates that the relative content of clay minerals in the mineral matter of net light coal is higher than that in the mineral matter of raw coal. The XRD patterns also support this observation. Compared to the LTA of the raw coal, the LTA of the preheated light coal contains less quartz. Additionally, the LTA of the net light coal still contains trace amounts of calcite and pyrite. However, these amounts are much less than those in the LTA from the raw coal. The potassium, magnesium and sodium contents are also quite low in the 815 °C ash of the WX net light coal.

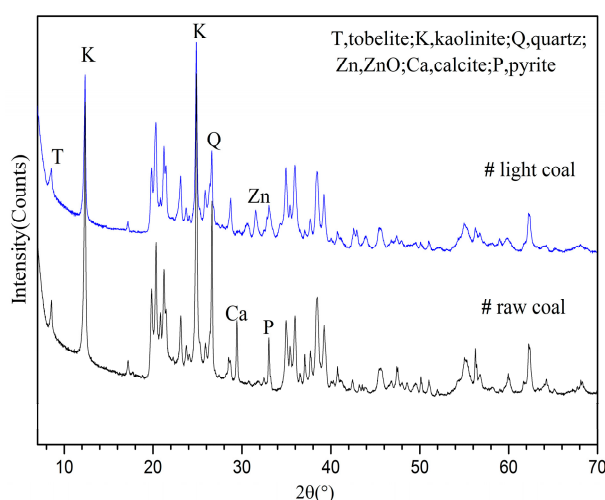


Figure 1. XRD patterns of LTA of WX raw and preheated WX light coal.

The SH light coal LTA contains quartz and clay minerals, but no feldspars are observable in the light coal LTA as compared with that in the raw coal LTA (Figure 3). As in the WX light coal, the mass ratio between kaolinite and muscovite in the SH light coal is the same as that in the SH raw coal. No Zn-bearing minerals, other than zinc oxide, are observable in the preheated SH light coal LTA.

The 815 °C ash sample of the SH net light coal has an aluminium content higher than that of the SH raw coal (Figure 2), indicating there are more clay minerals in net light coal mineral matter than in raw coal mineral matter.

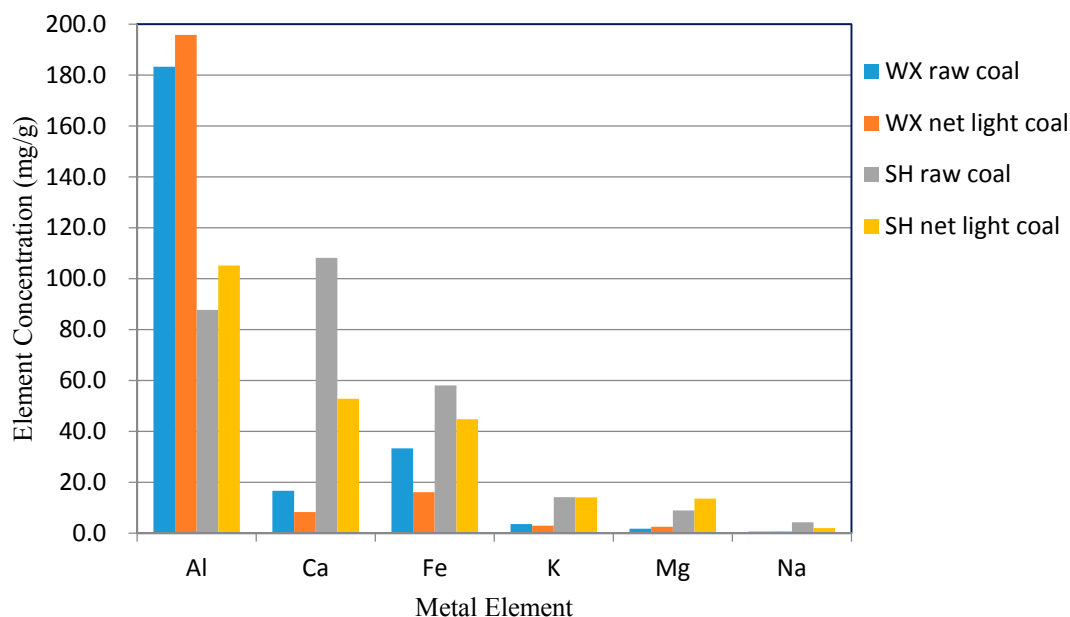


Figure 2. Major metal concentrations in 815 °C ash of raw coals and net light coals determined by ICP-AES (Left, WX coal ash; Right, SH coal ash).

Figure 3 shows a small amount of calcite in the preheated SH light coal LTA. The presence of bassanite ($\text{CaSO}_4 \cdot 0.5(\text{H}_2\text{O})$) suggests that SH light coal contains some organically-bound calcium [35]. Figure 2 demonstrates that the calcium content in the net light coal ash is much lower than that in the raw coal ash. The iron content in the SH net light coal ash is also lower than that in the SH raw coal ash, still 44.8 mg/g, although it was not identified by XRD analysis. The ash samples of SH coal have higher potassium contents than the WX coal ash does, due to potassium-bearing muscovite. Additionally, the SH coal ash contains small amounts of magnesium and sodium, whose contents are higher than they are in WX coal ash. These active metal elements can contribute to the production of high-NBO/T matter in the thermal reactions of clay minerals during coal combustion.

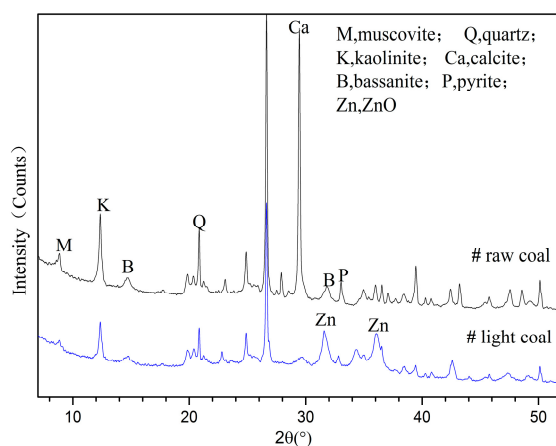


Figure 3. XRD patterns of LTA of SH raw and preheated SH light coal.

3.2. Phase Analyses of DTF Ashes and Their Boiling Acid Separation Residues

The phase components in the DTF ashes were analysed by comparing the XRD patterns of the DTF and MF ash samples. Comparison of DTF and MF ash can be employed to determine the phases in DTF ash samples reliably and can indicate the extent of the thermal reactions of clay minerals in light coal. Only the XRD patterns of the ash samples prepared at 1050 and 1250 °C are shown, for clarity.

3.2.1. Phase Analyses of SH Light Coal DTF Ash

For the SH light coal, the mineral distribution of DTF ash was significantly different from that of MF ash (Figure 4). The major minerals in the MF ash are willemite (Zn_2SiO_4) and hercynite ($FeAl_2O_4$), with a small amount of quartz. The two new minerals originated from the reactions of ZnO with the original mineral matter during the MF combustion process. In contrast, the major minerals in the DTF ash are zinc oxide and quartz, with a small amount of willemite.

One new zinc-bearing mineral, which was not dissolved by hydrochloric acid, was produced in the SH light coal DTF ash. This mineral is not easily distinguishable in the DTF ash XRD pattern because its diffraction peaks are close to those of zinc oxide. However, the diffraction peaks are clearly observable in the XRD pattern from the boiling acid separation residues of the DTF ash, where the zinc oxide was removed by hydrochloric acid (Figure 5). By searching the XRD phase database PDF2004, this new mineral was determined to be a zinc-bearing hercynite with the chemical formula $Zn_{0.4}Fe_{0.6}Al_2O_4$, based on the relationship between the structural parameters and the Fe-to-Zn ratio provided by Waerenborgh *et al.* [36]. Since hercynite has a high melting point of 1740 °C [37], the new mineral also has a high melting point. The production of this mineral proves that zinc oxide was involved in clay mineral reactions during DTF combustion of the SH light coal.

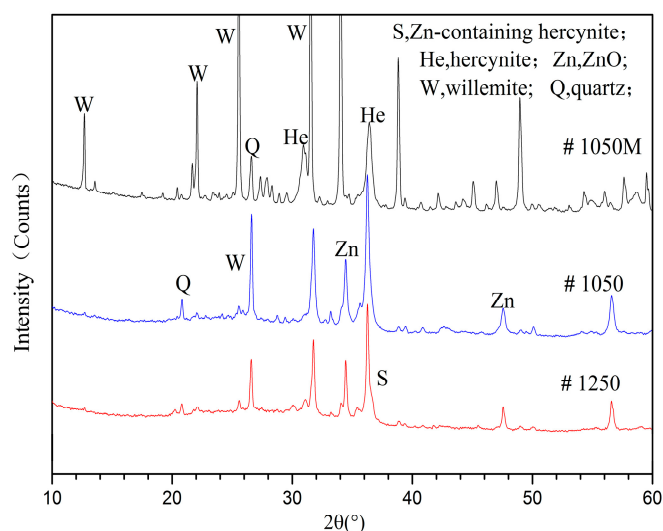


Figure 4. XRD patterns for 1050 and 1250 °C DTF ash (blue, red, respectively) and 1050 °C MF ash (black) of SH light coal.

As in the previous investigation of raw coal DTF ash [18], the amorphous aluminosilicates in the DTF ash residues after boiling acid separation were examined by analysing the diffuse diffraction humps in the XRD patterns of the DTF ash residues (Figures 6 and 7). For the XRD patterns to have the same baseline, thereby enabling comparison of the diffraction humps, the instrument background was subtracted. Moreover, the diffraction intensity per unit length was reduced in the vertical direction to emphasize the shapes of the diffraction humps.

In the XRD pattern of the 1250 °C DTF ash of SH light coal, the diffuse diffraction hump caused by glasses in the boiling-acid separation residues is symmetric, with a maximum at 22.7° 2θ (Figure 6).

This diffuse diffraction hump is identical to that of the glasses from the boiling acid separation residues of the SH raw coal DTF ash. Such a diffraction hump indicates that the aluminosilicate glasses in the boiling-acid separation residues had chemical structures similar to that of silica gel, a low-NBO/T amorphous material [18,23]. For the 1050 °C DTF ash, the diffuse diffraction hump of the boiling-acid separation residue has its maximum skewed to a higher 2θ diffraction angle, due to a certain amount of unburned carbon in the DTF ash.

Additionally, since the zinc oxide was dissolved in the acid, the original quartz and newly generated zinc-bearing hercynite were the major minerals in the DTF ash residues of the SH light coal. A small amount of mullite was also identified in the DTF ash residues of the SH light coal. The zinc-bearing hercynite in the 1250 °C DTF ash residue had more intense diffraction peaks than it did in the 1050 °C DTF ash residue, indicating that increasing the DTF temperature promoted the production of Zn-bearing hercynite.

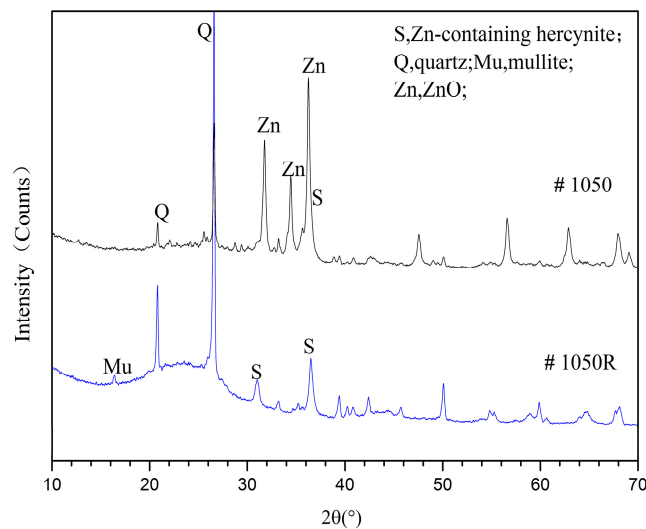


Figure 5. XRD patterns for 1050 °C DTF ash (black) of SH light coal and its boiling acid separation residue (blue).

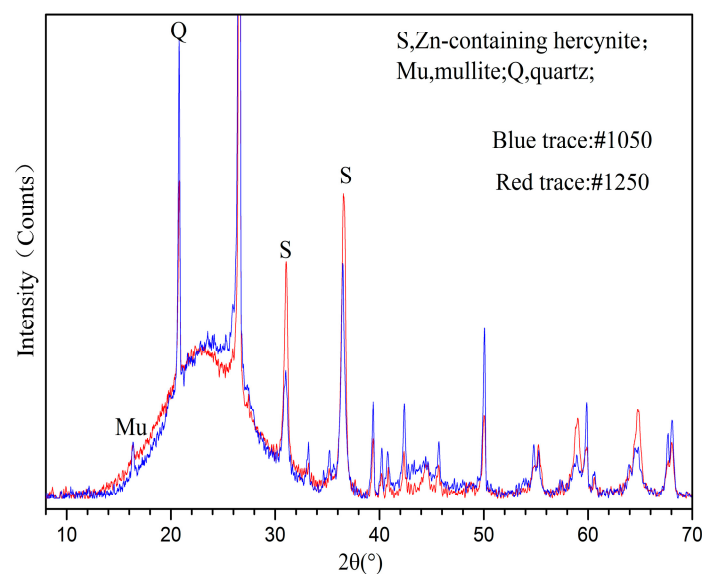


Figure 6. XRD patterns for boiling acid separation residues of 1050 and 1250 °C DTF ash of SH light coal.

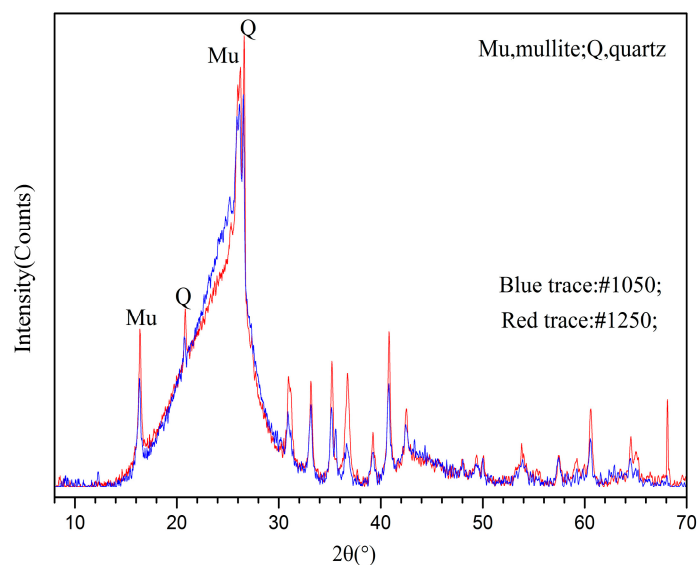


Figure 7. XRD patterns for boiling acid separation residues of 1050 and 1250 °C DTF ash of WX light coal.

The XRD analysis results prove that after boiling acid separation, the reaction products of clay minerals in DTF ash residues consist mostly of low-NBO/T matter with a structure similar to that of amorphous silica as well as a small amount of high-melting-point minerals.

3.2.2. Phase Analyses of WX Light Coal DTF Ash

For the WX light coal, the mineral distribution in DTF ash is largely different from that in MF ash (Figure 8). The MF ash lacks amorphous matter; its major minerals are gahnite, willemite and cristobalite. These new minerals originated from the reactions of ZnO with the original mineral matter. Additionally, the MF ash still contains a small amount of quartz. However, the major minerals in the WX light coal DTF ash are zinc oxide, mullite and quartz, all with relatively low XRD intensities. None of the major minerals in the MF ash exists in the DTF ash. The XRD patterns of the WX light coal DTF ash have single diffuse diffraction hump. The diffuse diffraction hump of the 1250 °C DTF ash is smaller than that of the 1050 °C DTF ash, indicating that increasing the DTF temperature reduces the amount of amorphous matter in WX DTF ash.

After treating the DTF ash of the WX light coal by boiling-acid separation, the diffuse diffraction humps of the ash residues are skewed towards higher 2θ diffraction angles (Figure 7). Such diffuse diffraction humps are also observable in the XRD curves of the DTF ash residue of the WX raw coal, as discussed by Tian *et al.* [18]. The WX coal, as a low-volatile bituminous coal, was difficult to burn out, and its DTF ash contains a significant amount of unburned carbon. These diffuse diffraction humps resulted from the superposition of diffuse diffractions caused by amorphous aluminosilicates and unburned carbon in DTF ash residues. With the same curve decomposition method, the XRD patterns for the DTF ash residues of this light coal demonstrate that aluminosilicate glasses have the same diffuse diffraction hump as silica gel, a representative low-NBO/T amorphous material. The diffuse diffraction hump in the XRD pattern for the residue of the 1250 °C DTF ash is slightly lower than the pattern from the residue of the 1050 °C DTF ash, since higher DTF temperature leave less unburned carbon. The loss on ignition (LOI) of an ash sample represents the unburned carbon content in the ash. The LOI values of the WX light coal DTF ash are higher than those of the SH light coal DTF ash, and with increasing DTF temperature, the LOI decreases (Table 3). Additionally, with the zinc oxide removed by boiling acid separation, the quartz and mullite were retained in the DTF ash residues of the WX light coal. Moreover, the mullite content in the DTF ash residue increases as the DTF temperature increases.

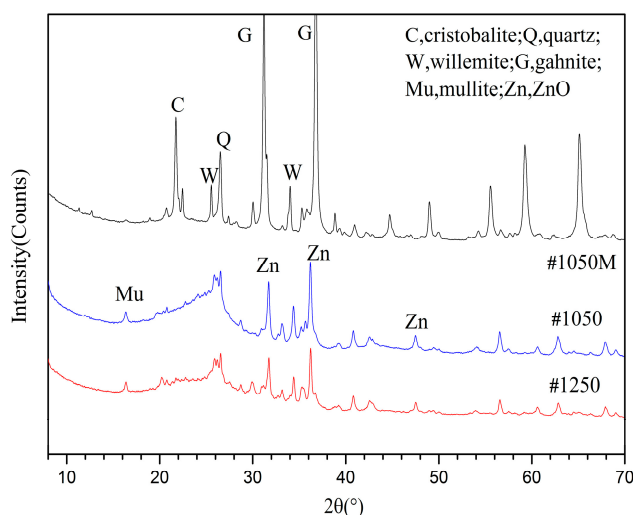


Figure 8. XRD patterns for 1050 and 1250 °C DTF ash and 1050 °C (#1050 M) MF ash of WX light coal.

Table 3. Loss on ignition (LOI) values of light coal drop-tube furnace (DTF) ash samples.

Sample	LOI	Sample	LOI
SHL 1050	0.15	WXL 1050	0.57
SHL 1150	0.09	WXL 1150	0.41
SHL 1250	0.06	WXL 1250	0.28

The XRD results for the DTF ash residues of the WX and SH light coal show that amorphous aluminosilicates in these samples were the low-NBO/T matter. Mullite and Zn-bearing hercynite in DTF ash residues are high-melting-point minerals which cannot cause boiler slagging. Thus, the acid-soluble aluminium fractions of the DTF ash samples represent the total fractions of dehydroxylation products and high-NBO/T matter in the thermal reaction products of the clay minerals in the two light coals.

3.3. Clay Mineral Reaction Characteristics in Light Coal DTF Ash

3.3.1. Reactions of ZnO with Clay Minerals

The reaction extents of the clay minerals in the MF combustion experiments were close to thermodynamic equilibrium. The XRD analysis results show that zinc oxide actively participated in the clay mineral reactions in the MF ash of the two light coals. The cristobalite in coal ash is transformed by amorphous silicon oxide, and the amorphous silicon oxide results from thermal decomposition of clay minerals in coal [38]. The existence of cristobalite in the WX light coal MF ash indicates that the clay minerals were sufficient to react with the other mineral matter in the coal sample. In contrast, the lack of cristobalite and the reduction of the original quartz in the SH light coal MF ash suggests that the zinc oxide was adequate to react with the clay minerals in this coal sample.

For the DTF combustion experiments, zinc chloride hydrate, introduced by ZnCl₂-solution density separation, completely decomposed to produce zinc oxide. However, the newly produced ZnO reacted weakly with the original clay minerals in the light coals. No Zn-bearing crystalline phases other than zinc oxide were in the WX light coal DTF ash. Mainly, self-transforming reactions occurred for the clay minerals in the light coal. Although a small amount of Zn-bearing hercynite was produced by the clay mineral thermal reactions, zinc oxide was still the most abundant Zn-bearing phase in the SH light coal DTF ash.

Additionally, the properties of the organic matter in coal should influence the reactions of zinc oxide with clay minerals during DTF combustion. In MF heating, the zinc oxide reacts completely with

the clay minerals in WX and SH light coals. WX light coal has a higher mineral matter content than SH light coal. In this experiment, with DTF combustion, some Zn-bearing hercynite was generated in the SH light coal DTF ash, while no new Zn-bearing crystalline substance was produced in the WX light coal DTF ash. This result is related to differences between the types of organic matter in these two fuels. During pulverized coal combustion, the char particles of different macerals fragment and burnout in different ways, influencing the ash formation and the included minerals [9,10]. The organic components of SH coal, a highly volatile bituminous coal, should contribute more to the combination of clay minerals and zinc oxide than the organic components of WX low-volatile bituminous coal contribute. Since the zinc oxide could react with the clay minerals to produce crystalline compounds such as the Zn-bearing hercynite, some Zn-bearing aluminosilicate glass was surely in the DTF ash samples. During silicate reactions, ferrous oxide is similar to zinc oxide. In view of the performance of zinc oxide, extraneous ferrous oxide should react with clay minerals in coal during pulverized coal combustion, although possibly only slightly. Additionally, the organic components of coal should also affect the interaction of ferrous oxide with clay minerals in coal.

3.3.2. Comparison of Clay Mineral Reaction Products between Light Coals and Raw Coals

For WX and SH raw coal, previous reports discussed [18] how components of the acid-soluble products of clay minerals changed with increasing DTF temperature. In this study, the clay minerals in the WX raw coal essentially transformed themselves during DTF combustion. For the WX raw coal, increasing the DTF temperature from 1050 to 1150 °C prompted dramatic mullite-producing reconversion of the dehydroxylation products of the clay minerals (Figure 9). The DTF temperature slightly affected the reconversion in the DTF temperature range from 1150 to 1250 °C.

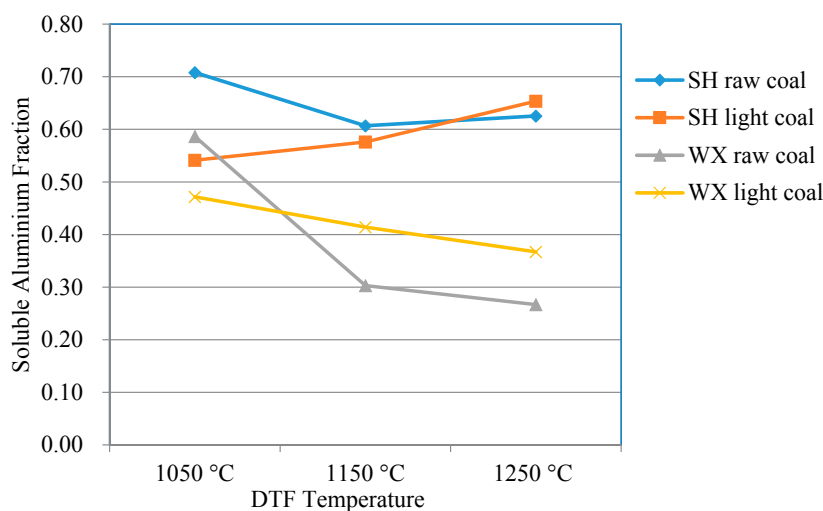


Figure 9. Soluble aluminium fractions in DTF ashes of SH and WX coal.

For the WX light coal, the results of the XRD analysis of its DTF ash imply that the clay minerals mainly underwent self-reactions during DTF combustion. In Figure 9, the downward trend in the soluble aluminium fraction of the WX light coal DTF ash also demonstrates the thermal self-transformation characteristics of the clay minerals in the WX light coal. The soluble aluminium fraction of the 1050 °C DTF ash of the WX light coal is less than that of the WX raw coal ash at the same DTF temperature. The acid-solubility of aluminium in the dehydroxylation products of kaolinite is related to the degree of dehydroxylation [26]. The dehydroxylation reactions of the clay minerals in WX light coal should be incomplete at a DTF temperature of 1050 °C.

Moreover, the soluble aluminium fraction of the WX light coal DTF ash decreases steadily as the DTF temperature increases from 1050 to 1250 °C. The features of the clay mineral products in the

WX light coal ash samples should be due to the different maceral concentrations of WX light coal and WX raw coal. Compared to WX raw coal, WX light coal has a higher maceral concentration, and its clay mineral particles are wrapped more inside the organic matter. As a low volatile bituminous coal, WX coal is low in volatile matter and rich in coke. There were large amounts of unburned carbon in the WX light coal DTF ash samples. The unburned carbon particles hindered the thermal self-transforming reactions of the clay minerals. The light coal carried a small amount of zinc chloride hydrate; its endothermic decomposition could occur at 200 °C. The decomposition reaction might delay the heating of coal particles to some extent but should not be a main factor in hindering the self-transformation of clay minerals.

An important observation is that the 1250 °C DTF ash of the WX light coal has a higher soluble aluminium fraction than that of the WX raw coal has, indicating that this sample had more dehydroxylation products of clay minerals than the raw coal ash sample at the same DTF temperature had. When light coal burns in a utility boiler, the dehydroxylation products can combine with other extraneous metal oxides at the ash deposition positions, although there is no zinc oxide in the boiler furnace. These combination reactions occur more easily than the combination of mullite with extraneous metal oxides.

With SH coal samples burning in a DTF, the clay minerals self-react and react with active metal oxides derived from the fuels. In this study, for the SH light coal, the soluble aluminium fraction of the 1050 °C DTF ash is less than that of the SH raw coal ash at the same DTF temperature (Figure 9), as explained for WX light coal. That is, at this DTF temperature, the dehydroxylation reactions of the clay minerals were not completed. However, the soluble aluminium fraction increases as the DTF temperature increases from 1050 to 1250 °C. The soluble aluminium fraction of the WX light coal DTF ash decreases with increasing temperature in this temperature range. This difference proves that increasing the DTF temperature prompts the dehydroxylation products of clay minerals in SH light coal to generate high-NBO/T matter.

For the SH raw coal [18], the soluble aluminium fraction of its DTF ash first decreases slowly, then increases slightly over the whole DTF temperature range from 1050 to 1250 °C. The difference between the DTF ash of the SH light coal and the SH raw coal indicates that the DTF temperature promotes the production of high-NBO/T matter in SH light coal ash. The SH light coal starts to produce more high-NBO/T matter than the SH raw coal produces at a DTF temperature of 1250 °C. When SH coal is used as a fuel in utility boiler furnaces, its light coal fraction carries no zinc chloride hydrate and is the net light coal. The combustion temperatures are usually higher than 1250 °C in boiler furnaces. The higher combustion temperatures must promote positive interactions between the clay minerals and the metal elements derived from the original mineral matter. Thus, the clay minerals in SH net light coal will produce a significant amount of high-NBO/T matter on the ash deposition positions, playing an important role in the occurrence of boiler slagging.

4. Conclusions

The light fractions of two Chinese coals were prepared using a $1.5 \text{ g} \cdot \text{cm}^{-3}$ ZnCl_2 solution as a density separation medium and were burned in a drop-tube furnace (DTF). The acid-soluble aluminium fractions of DTF ash samples were used to determine changes in the amorphous aluminosilicate products. The key findings from these studies are as follows:

- (1) The content of clay minerals in the mineral matter of net light coals is higher than that in the relevant raw coals. Thermal reactions of clay minerals should be the focal point of investigations of production mechanisms for easily-slagging material in the ash of light coal fractions.
- (2) For WX coal with a high ash melting point, increasing the DTF temperature resulted in more dehydroxylation products of the clay minerals in the ash of light coal compared to in the ash of raw coal. The dehydroxylation products will contribute to the solid-state reactions of ash particles.
- (3) For SH coal with a low ash melting point, increasing the DTF temperature had a more significantly positive impact on the production of high-NBO/T matter in the ash of light coal compared to in

the ash of raw coal. In utility boiler furnaces, the clay minerals in light coal will play an important role in the occurrence of slagging.

- (4) Extraneous zinc oxide, formed by introduction from a zinc chloride solution, was found to react slightly with the clay minerals in the light coal fractions during DTF combustion. The organic components derived from highly volatile SH coal may contribute more to the interaction of zinc oxide with clay minerals than those derived from less-volatile WX coal contribute.

Acknowledgments: This research was supported by the National Science Foundation of China (No. 51376061). The support of the China Scholarship Council for the first author is greatly appreciated. We also gratefully acknowledge Changhe Chen for the advice regarding the experimental work and Eric Eddings for the initial review on the manuscript.

Author Contributions: Sida Tian and Yuqun Zhuo conceived and designed the experiments. Sida Tian and Xinqian Shu finished the experiments. Sida Tian, Zhonghua Zhan and Yuqun Zhuo wrote the manuscript. Zhizhong Kang provided some ideas on the paper.

Conflicts of Interest: The authors declare no conflict of interest.

References

1. Bryers, R.W. Fireside slagging, fouling, and high temperature corrosion of heat-transfer surface due to impurities in steam-raising fuels. *Prog. Energy Combust. Sci.* **1996**, *22*, 29–120. [[CrossRef](#)]
2. Creelman, R.A.; Ward, C.R.; Schumacher, G.; Juniper, L. Relation between coal mineral matter and deposit mineralogy in pulverized fuel furnaces. *Energy Fuels* **2013**, *27*, 5714–5724. [[CrossRef](#)]
3. Shen, M.; Qiu, K.; Zhang, L.; Huang, Z.; Wang, Z.; Liu, J. Influence of coal blending on ash fusibility in reducing atmosphere. *Energies* **2015**, *8*, 4735–4754. [[CrossRef](#)]
4. Benson, S.A.; Jones, M.L.; Harb, J.N. Ash Formation and Deposition. In *Fundamentals of Coal Combustion for Clean and Efficient Use*; Smoot, L.D., Ed.; Elsevier: New York, NY, USA, 1993; pp. 299–373.
5. Zhang, Z.; Wu, X.; Zhou, T.; Chen, Y.; Hou, N.; Piao, G.; Kobayashid, N.; Itayad, Y.; Morid, S. The effect of iron-bearing mineral melting behaviour on ash deposition during coal combustion. *Proc. Combust. Inst.* **2011**, *33*, 2853–2861. [[CrossRef](#)]
6. Reinmüller, M.; Klinger, M.; Schreiner, M.; Gutte, H. Relationship between ash fusion temperatures of ashes from hard coal, brown coal, and biomass and mineral phases under different atmospheres: A combined FactSage™ computational and network theoretical approach. *Fuel* **2015**, *151*, 118–123. [[CrossRef](#)]
7. Gupta, R.P.; Wall, T.F.; Kajigaya, I.; Miyamae, S.; Tsumita, Y. Computer-controlled scanning electron microscopy of minerals in coal—Implications for ash deposition. *Prog. Energy Combust. Sci.* **1998**, *24*, 523–543. [[CrossRef](#)]
8. Russell, N.V.; Mendez, L.B.; Wigley, F.; Williamson, J. Ash deposition of a Spanish anthracite: Effect of included and excluded mineral matter. *Fuel* **2002**, *81*, 657–663. [[CrossRef](#)]
9. Hurley, J.P.; Schobert, H.H. Ash formation during pulverized subbituminous coal combustion. 2. Inorganic transformations during middle and late stages of burnout. *Energy Fuels* **1993**, *7*, 542–553. [[CrossRef](#)]
10. Wu, H.; Wall, T.; Liu, G.; Bryant, G. Ash liberation from included minerals during combustion of pulverized coal: The relationship with char structure and burnout. *Energy Fuels* **1999**, *13*, 1197–1202. [[CrossRef](#)]
11. Spears, D.A.; Martinez-Tarazon, M.R. Geochemical and mineralogical characteristics of a power station feed-coal, Eggborough, England. *Int. J. Coal Geol.* **1993**, *22*, 1–20. [[CrossRef](#)]
12. Shimogori, M.; Mine, T.; Ohyatsu, N.; Takarayama, N.; Matsumura, Y. Effects of fine ash particles and alkali metals on ash deposition characteristics at the initial stage of ash deposition determined in 1.5 MW pilot plant tests. *Fuel* **2012**, *97*, 233–240. [[CrossRef](#)]
13. Russell, N.V.; Wigley, F.; Williamson, J. The roles of lime and iron oxide on the formation of ash and deposits in PF combustion. *Fuel* **2002**, *81*, 673–681. [[CrossRef](#)]
14. Wee, H.L.; Wu, H.; Zhang, D. Heterogeneity of ash deposits formed in a utility boiler during PF combustion. *Energy Fuels* **2007**, *21*, 441–450. [[CrossRef](#)]
15. Barroso, J.; Ballester, J.; Pina, A. Study of coal ash deposition in an entrained flow reactor: Assessment of traditional and alternative slagging indices. *Fuel Process. Technol.* **2007**, *88*, 865–876. [[CrossRef](#)]

16. Zhang, J.; Zhao, Y.; Wei, C.; Yao, B.; Zheng, C. Mineralogy and microstructure of ash deposits from the Zhuzhou coal-fired power plant in China. *Int. J. Coal Geol.* **2010**, *81*, 309–319. [[CrossRef](#)]
17. Lee, B.; Kim, S.I.; Kim, S.M.; Oh, D.H.; Gupta, S.; Jeon, C. Ash deposition characteristics of Moolarben coal and its blends during coal combustion. *Korean J. Chem. Eng.* **2016**, *33*, 147–153. [[CrossRef](#)]
18. Tian, S.; Zhuo, Y.; Chen, C. Characterization of the products of the clay mineral thermal reactions during pulverization coal combustion in order to study the coal slagging propensity. *Energy Fuels* **2011**, *25*, 4896–4905. [[CrossRef](#)]
19. Ward, C.R.; French, D. Determination of glass content and estimation of glass composition in fly ash using quantitative X-ray diffractometry. *Fuel* **2006**, *85*, 2268–2277. [[CrossRef](#)]
20. Vargas, S.; Frandsem, F.J.; Dam-Johansen, K. Rheological properties of high-temperature melts of coal ashes and other silicates. *Prog. Energy Combust. Sci.* **2001**, *27*, 237–429. [[CrossRef](#)]
21. Lu, P. *Fundamentals of Inorganic Materials Science (Chemistry and Physics of Silicates)*; Wuhan University of Technology Press: Wuhan, China, 2006; pp. 77–106. (In Chinese)
22. Mysen, B.O. Element partitioning between mineral and melt, melt composition, and melt structure. *Chem. Geol.* **2004**, *213*, 1–16. [[CrossRef](#)]
23. Berry, E.E.; Hemmings, R.T.; Cornelius, B.J. Speciation in size and density fractionated fly ash III the influence of HCl leaching on the glassy constituents of a high-Ca fly ash. *Mater. Res. Soc. Symp. Proc.* **1988**, *113*, 55–63. [[CrossRef](#)]
24. Toplis, M.J.; Dingwell, D.B. Shear viscosities of CaO-Al₂O₃-SiO₂ liquids: Implications for the structural role of aluminium and the degree of polymerization of synthetic and natural aluminosilicate melts. *Geochim. Cosmochim. Acta* **2004**, *68*, 5169–5188. [[CrossRef](#)]
25. Kuo, Y.; Huang, K.; Wang, C.; Wang, J. Effect of Al₂O₃ mole fraction and cooling method on vitrification of an artificial hazardous material. Part 1: Variation of crystalline phases and slag structures. *J. Hazard. Mater.* **2009**, *169*, 626–634. [[CrossRef](#)] [[PubMed](#)]
26. Belver, C.; Munoz, M.A.B.; Vicente, M.A. Chemical activation of a Kaolinite under acid and alkaline conditions. *Chem. Mater.* **2002**, *14*, 2033–2043. [[CrossRef](#)]
27. Zhao, Y.; Zhang, J.; Sun, J.; Bai, X.; Zheng, C. Mineralogy, chemical composition, and microstructure of ferrospheres in fly ashes from coal combustion. *Energy Fuels* **2006**, *20*, 1490–1497. [[CrossRef](#)]
28. Yang, J.; Zhao, Y.; Zyryanov, V.; Zhang, J.; Zheng, C. Physical-chemical characteristics and elements enrichment of magnetospheres from coal fly ashes. *Fuel* **2014**, *135*, 15–26. [[CrossRef](#)]
29. Terry, B. Acid decomposition of silicate minerals. Part I: Reactivities and modes of dissolution of silicates. *Hydrometallurgy* **1983**, *10*, 135–150. [[CrossRef](#)]
30. Behrens, H.; Haack, M. Cation diffusion in soda-lime-silicate glass melts. *J. Non-Cryst. Solids* **2007**, *353*, 4743–4752. [[CrossRef](#)]
31. Jones, F.; Bankiewicz, D.; Hupa, M. Occurrence and sources of zinc in fuels. *Fuel* **2014**, *117*, 763–775. [[CrossRef](#)]
32. Tian, S.; Zhuo, Y.; Shu, X.; Chen, C.; Li, D. Distribution of mineral matter in Shenhua coal by combined ZnCl₂ and HCl fractionation. *J. Tsinghua Univ. Sci. Technol.* **2008**, *48*, 240–243. (In Chinese)
33. *Determination of Fusibility of Coal Ash*; GB/T 219-2008; China National Standard: Beijing, China, 2008.
34. *Proximate Analysis of Coal*; GB/T 212-1991; China National Standard: Beijing, China, 1991.
35. Tian, S.; Zhuo, Y.; Shu, X.; Chen, C. The chemical transformation of calcium in Shenhua coal during combustion in a muffle furnace. In Proceedings of the 7th International Symposium on Coal Combustion, Harbin, China, 17–19 July 2011.
36. Waerenborgh, J.C.; Figueiredo, M.O.; Cabral, J.M.; Pereira, L. Powder XRD structure refinements and ⁵⁷Fe Mossbauer effects study of synthetic Zn_{1-x}Fe_xAl₂O₄ (0 < x ≤ 1) spinels annealed at different temperatures. *Phys. Chem. Miner.* **1994**, *21*, 460–468.
37. Fukushima, J.; Hayashi, Y.; Takizawa, H. Structure and magnetic properties of FeAl₂O₄ synthesized by microwave magnetic field irradiation. *J. Asian Ceram. Soc.* **2013**, *1*, 41–45. [[CrossRef](#)]
38. Mollah, M.; Promreuk, S.; Schennach, R.; Cocke, D.; Guler, R. Cristobalite formation from thermal treatment of Texas lignite fly ash. *Fuel* **1999**, *78*, 1277–1282. [[CrossRef](#)]

